

# BSIM3v3 based Degradation Compact Model for Circuit Simulation of Non-Volatile Flash Memories

F. Schuler<sup>1,2</sup>, O. Kowarik<sup>1</sup>, K. Hoffmann<sup>1</sup>

<sup>1</sup> University of Bundeswehr Munich, ET4, Werner-Heisenberg-Weg 39, D-85577 Neubiberg,  
phone: +49/89/6004-3662, fax: -2223, Franz.Schuler@unibw-muenchen.de

<sup>2</sup> now: Siemens AG, Semiconductor Group, Balanstr. 73, D-81541 Munich

**Abstract** — A BSIM3v3.1 based flash memory degradation compact model for circuit simulators has been developed. By a physics based modification of the Fowler-Nordheim equation the tunnel current can be calculated considering both positive and negative oxide charges. It has been shown, that every known endurance characteristic can be simulated by this model. It allows a precise simulation of worst case operation of flash memories and an optimized circuit design.

## I. Introduction

Oxide traps are generated by Fowler-Nordheim tunneling of electrons. These traps can be charged positively or negatively [1,2]. Positive oxide charges improve the tunnel current and the  $V_T$ -window (fig.1, sections I), negative ones decrease the tunnel current and the  $V_T$ -shift (fig.1, sections II).

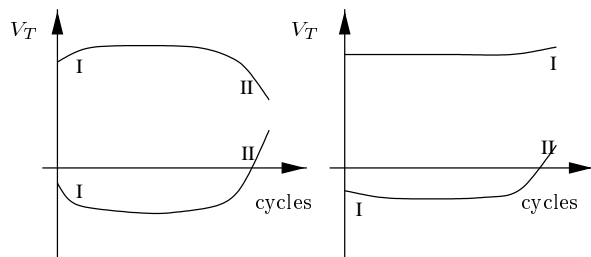


Fig. 1: Different endurance schematics for NAND flash memories known from literature [1,3-7].

However, so far proposed degradation models consider only the influence of negative oxide charges [8,9] or of positive charges only in the channel region [1].

In this work a improved physics based tunnel current model for circuit simulation is proposed taking both negative and positive oxide charges in all regions into account.

## II. Theory

The theory behind our model can be explained by fig.2 and fig. 3. The flash memories are programmed by electrons, which tunnel from the source and/or drain to the floating gate by applying a positive control gate voltage (fig. 2a). They are erased by electrons tunneling from the floating gate to the substrate resulting from a negative control gate voltage or a positive substrate voltage (source and drain floating) (fig. 3a). Thus, we have two different tunnel oxides for programming and erasing with different aging parameters.

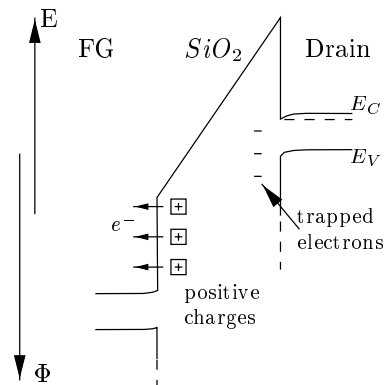
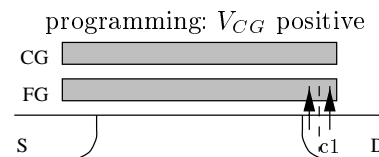


Fig. 2: a) Programm schematic  
b) Band diagram: cross-section c1

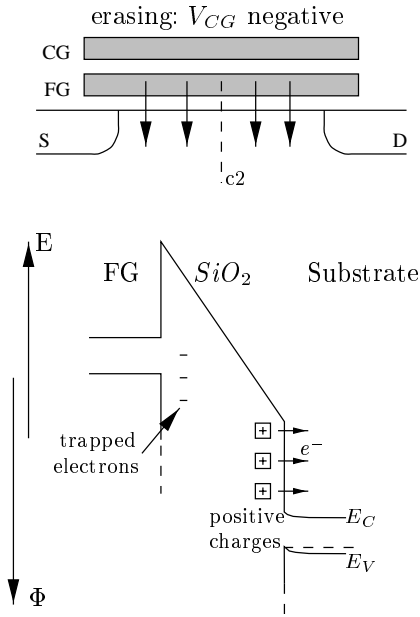


Fig. 3: a) Erase schematic  
b) Band diagram: cross-section c2

Applying high voltages to an oxide there are two basic effects creating oxide charges:

1. Tunneling electrons are trapped by existing oxide traps.
2. Positive oxide charges are generated by de-trapping of electrons.

This is sketched in fig. 2b and 3b.

### III. Model

The tunnel current through a triangular barrier can be described by the well-known Fowler-Nordheim equation

$$J_{tunnel} = A_1 E^2 e^{-\frac{A_2}{E}}$$

with the constants  $A_1$  and  $A_2$  and the electric field  $E$  in the oxide. However, the generated and trapped oxide charge change the band diagram and the electric field as shown in fig. 4. Thus, the description of the tunnel current has to be modified.

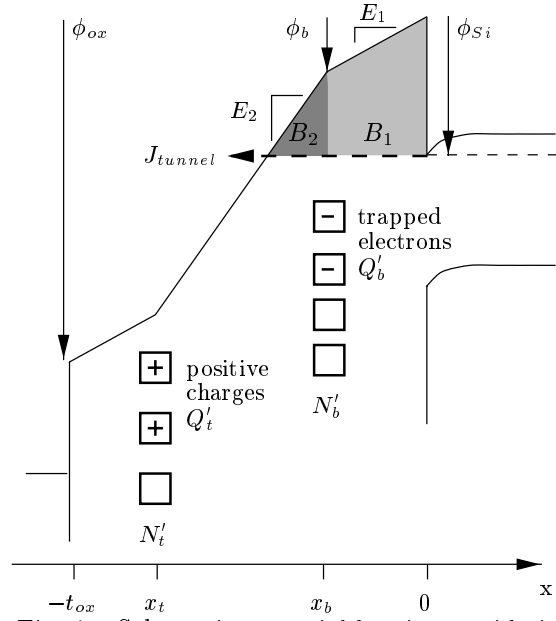


Fig. 4: Schematic potential barrier considering oxide charges.

Resulting from the WKB approximation [1], [8] and [9] calculate a modified tunnel current. However, they do not take positive oxide charges into account.

Considering both negative and positive charges the tunnel current can be described by

$$J_{tunnel} = C E_1^2 P_1 P_2$$

with

$$P_1 = \exp \left\{ -\frac{4}{3\hbar} \sqrt{2q m_{ox}} \frac{\phi_{Si}^{3/2} - (\phi_{Si} - \phi_b)^{3/2}}{E_1} \right\}$$

$$P_2 = \begin{cases} 1 & : \phi_b > \phi_{Si} \\ \exp \left\{ -\frac{4}{3\hbar} \sqrt{2q m_{ox}} \frac{(\phi_{Si} - \phi_b)^{3/2}}{E_2} \right\} & : \text{otherwise} \end{cases}$$

and

$$E_1 = \frac{\phi_{ox}}{t_{ox}} + \frac{1}{\epsilon} \left\{ Q'_b \left( 1 + \frac{x_b}{t_{ox}} \right) + Q'_t \left( 1 + \frac{x_t}{t_{ox}} \right) \right\}$$

$$E_2 = -\frac{Q'_b}{\epsilon} + E_1$$

$$\phi_b = -E_1 x_b.$$

$P_1$  describes the tunnel probability through the barrier  $B_1$  and  $P_2$  the tunnel probability through  $B_2$  (fig. 4).

So far it is not clear how the oxide charge change with respect to aging. Our model assumes the following rate description [12]

$$\begin{aligned}\frac{dQ'}{d\text{cycle}} &= \frac{\sigma}{q} J_{\text{tunnel}}(\text{cycle})(qN' - Q'(\text{cycle})) \\ Q'(\text{cycle}) &= qN' \left(1 - e^{-\frac{\text{cycle} \sigma J}{q}}\right) \\ &= qN' \left(1 - e^{-\frac{\text{cycle} \sigma J}{d_{\text{cycle} \epsilon}}}\right)\end{aligned}$$

where  $N'$  stands for the trap densities  $N'_b$  and  $N'_t$ ,  $Q'$  for the trapped charge  $Q'_b$  and  $Q'_t$ ,  $J$  for the average tunnel current and  $\sigma$  for the capture cross-section.

Fig. 5 demonstrates the influence of the charges  $Q'_b$  and  $Q'_t$  on the tunnel current while programming.

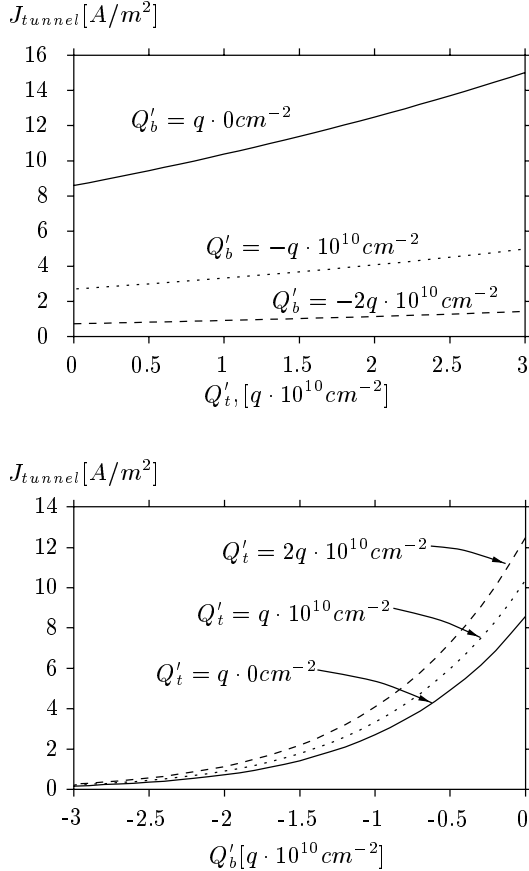


Fig. 5: Influence of the oxide charges  $Q'_b$  and  $Q'_t$  on the tunnel current during programming.

#### IV. Parameter extraction

The basic of the parameter extraction are the endurance characteristics. The strong  $V_T$  shift at the end of the endurance can be affected by charges near the injection side only, since charges at the other side have only a minor influence, since  $B_1$  and  $B_2$  are basically unchanged. Thus, the initial  $V_T$  shift must result from charges near the non-injection side. Since there are different tunnel oxides for programming and erasing the parameters  $N'$ ,  $d_{\text{cycle}}$  and the charge location may be different for programming and erasing for the injection side as well as for the non-injection side.

Using these easy to determine parameters one is able to simulate all known endurance characteristic [1,3-7].

#### V. Results

The degradation model has been implemented into the circuit simulator SABER using a BSIM3v3.1 based flash memory compact model.

Fig. 6a shows the control gate voltage while a programming-erasing-programming cycle and the resulting floating gate potential for different numbers of cycles. Fig. 6b demonstrates the corresponding tunnel currents for programming ( $I_{\text{tun},S \rightarrow FG}$ ,  $I_{\text{tun},D \rightarrow FG}$ ) and erasing ( $I_{\text{tun},FG \rightarrow B}$ ).

Observing the floating gate potential after erasing (cutline 1 in fig. 6a) and programming (cutline 2) the influence of trapped charges in the oxide is obvious (fig. 7). This results in a  $V_T$ -shift in the current characteristics shown in fig. 8.

From the current characteristics (fig. 8) the threshold voltages  $V_T$  can be determined. The resulting well-known endurance characteristics are shown in figure 9a. Different degradation parameters result in an endurance characteristic shown in fig. 9b. Thus, every known endurance behaviour can be simulated by the proposed degradation model. It also allows the optimization of circuit designs with respect to degradation effects.

#### VI. Conclusion

A compact flash memory degradation model has been developed. Thus, the circuit behaviour can be simulated depending on endurance characteristics. Mismatching between cells and cells/reference cells can be included into the circuit design.

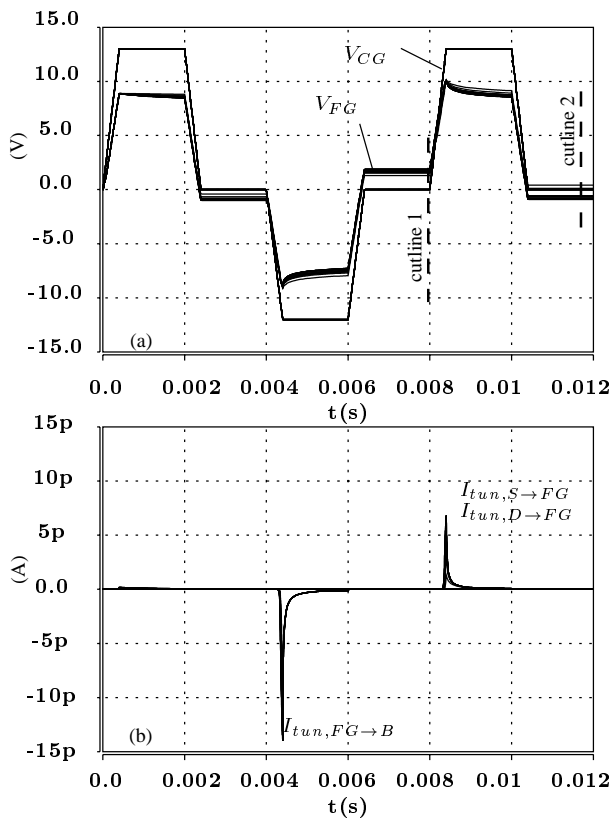


Fig. 6: Voltage and tunnel current behaviours while a programming-erasing-programming cycle.

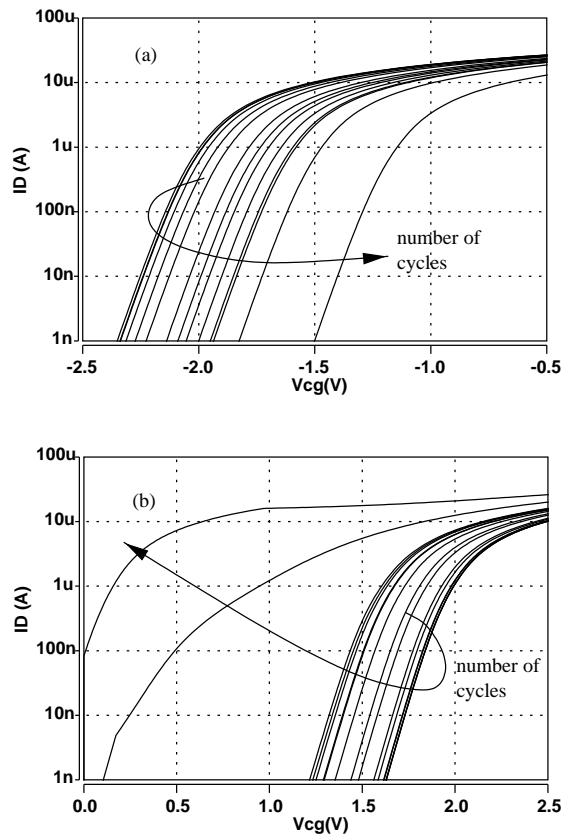


Fig. 8: Current characteristics for an erased (a) and programmed (b) NAND cell.

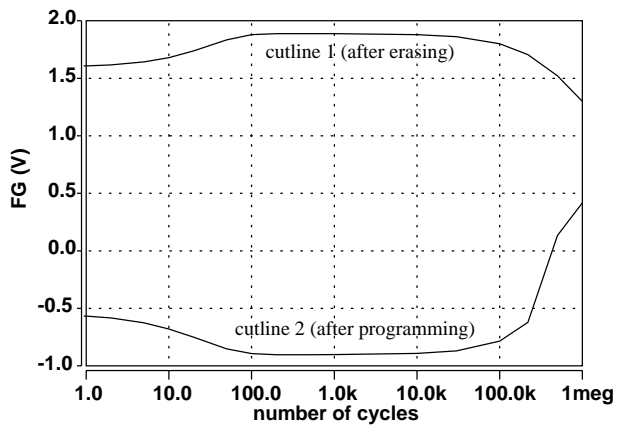


Fig. 7: Influence of charge trapping on the floating gate potential after erasing (cutline 1 in fig. 6a) and programming (cutline 2)

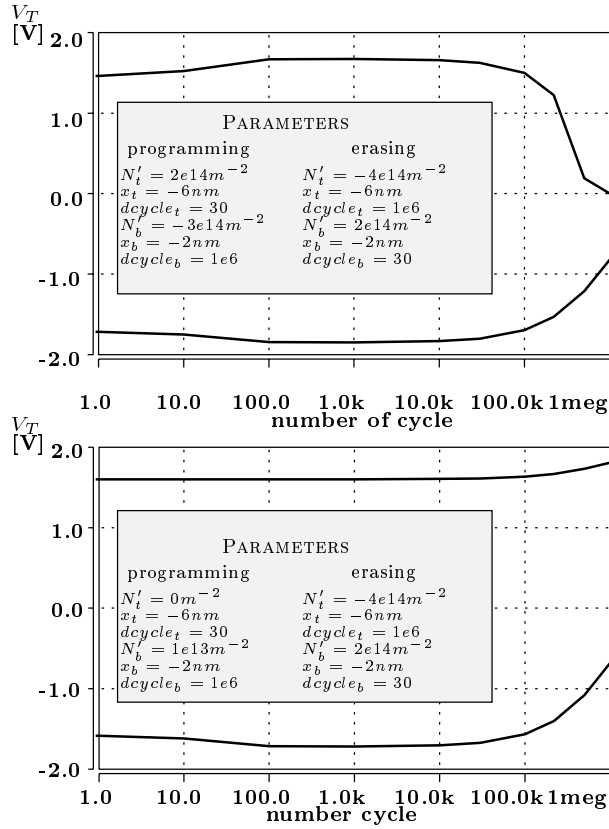


Fig. 9: Simulated  $V_T$  endurance for different aging parameters.

## References

- [1] J. S. Witters, G. Groeseneken, Herman E. Maes, IEEE Trans. Electr. Dev., ED-36, p. 1663, 1989
- [2] I.-C. Chen, S. E. Holland, and C. Hu, IEEE Trans. Electr. Dev., ED-32, p. 413, 1985
- [3] J.K. Yeh et al., ESSDERC Tech. Dig., p. 260, 1997
- [4] P.Cappelletti et al., IEEE IEDM Techn. Dig., p. 291, 1994
- [5] S. Aritome et al., IEEE IEDM Techn. Dig., p. 275, 1995
- [6] D.J. Kim et al., Symposium on VLSI Technology Digest of Techn. Papers, p. 236, 1996
- [7] S. Aritome et al. Proc. IEEE, vol. 81, no. 5, p.776, 1993
- [8] P.S. Ku, and D. K. Schroder, IEEE Trans. Electr. Dev., ED-41, p.1669, 1994
- [9] S. J. Oh and Y. T. Yeow, Solid-State Electronics, vol. 32, p. 507, 1989
- [10] T. Wang et al., Symposium on VLSI Technology Digest of Techn. Papers, p. 232, 1996
- [11] Takashi Hori, Symposium on VLSI Technology Digest of Techn. Papers, p. 69, 1990
- [12] M.S. Liang and C. Hu, IEEE IEDM Techn. Dig., p. 396, 1981

*This work was sponsored by the DFG (Ho 1325/2-2).*